LETTER REPORT

Cohesive Sediment Erosion Field Study: Kalamazoo River, Kalamazoo, Michigan

David W. Perkey, S. Jarrell Smith, and Thomas Kirklin

US Army Engineer Research and Development Center
Coastal and Hydraulics Laboratory
Vicksburg, Mississippi

24 April 2014

The U.S. Army Corps of Engineers (USACE) has a Pollution Removal Fund Authorization (PRFA # 34-13-463VXZ009) with the U.S. Environmental Protection Agency (EPA) to provide technical expertise and input regarding characterization and management of oil and oil contaminated sediments in the Kalamazoo River near Marshall, MI resulting from the July 26, 2010 oil spill. EPA has requested USACE to provide cohesive sediment erosion testing along a reach of the Kalamazoo River (in the vicinity of Marshall, MI). This report describes field experiments conducted to define cohesive sediment erosion processes of the contaminated sediment deposit and analysis of these data to parameterize cohesive sediment transport in the numerical sediment transport model.

Cohesive Sediment Transport Processes

The sediment bed within impounded areas of the Kalamazoo River (i.e. Morrow Lake and mill ponds upstream of Battle Creek Dam) impacted by the oil spill contains cohesive sediments. Non-cohesive sediment (sand and gravel) erosion and settling can be generally estimated from grain size distribution and mineral density. Cohesive sediment transport processes are dominated by other factors. Cohesive sediments are generally a mixture of sand, silt, and clay sized particles.

Erosion

A general definition for cohesive sediment is sediment for which the erosion rate cannot be estimated by standard sand/gravel transport methods. In these cases, cohesive forces are equivalent to or are greater than the gravitational forces that dominate sand transport. Cohesive sediment erosion characteristics are highly dependent upon factors such as particle size distribution, particle coatings, fine sediment mineralogy, organic content, bulk density, gas content, pore-water chemistry, and biological activity. Erosion rate and critical shear stress for erosion can vary significantly with small changes in only one of these inter-dependent parameters. It has been well demonstrated that critical stress and erosion rates for cohesive sediment can vary over several orders of magnitude for sediments with only slightly differing properties. Therefore, the influence of cohesion on sediment processes is significant. Qualitatively, it is understood which properties most significantly influence erosion. However, there are no quantitative methods available to determine erosion rate from cohesive sediment properties. Therefore, due to the sensitivity and wide range of influencing parameters, erosion characteristics of cohesive sediments are determined by site-specific analysis of erosion with erosion flumes.

Several flumes are available to parameterize site-specific cohesive sediment erosion algorithms. Most of these devices operate over a range of low shear stress (<2 Pa) and are consequently capable of measuring only surface sediment erosion. Sedflume is an erosion device with capability to impose bed stresses in the range of 0.1 to 12 Pa and measures erosion rates from sediment cores taken from the field (for in-situ or stratified bed conditions) or prepared in the laboratory (for assessing disturbed sediments such as dredged material). Sedflume is designed to quantify erosion rates for surface and sub-surface sediments. These measurements permit description of the vertical variation of erosion rate within the bed. It should be noted that even if sediments are well mixed, cohesive sediment bed erosion will change with depth due to the influence of consolidation (bed density) on erosion rate. Erosion rate can vary by several orders of magnitude between surficial sediments and sediment buried less than 30 cm below the surface. Sedflume was selected to quantify erosion rate and erosion rate variation with depth (density) for this study.

Methods

This section describes the field experiments, sampling and experimental methods, and data analysis methods used in determining cohesive sediment erosion in the Kalamazoo River in the vicinity of Marshall, MI. Background and technical information about the experimental device is presented first, followed by description of how these devices were deployed during field experiments to meet the study objectives.

Sedflume

Sedflume is a field- or laboratory-deployable flume for quantifying cohesive sediment erosion. The USACE-developed Sedflume is a derivative of the flume developed by researchers at the University of California at Santa Barbara (McNeil et al. 1996). The flume includes an 80-cm-long inlet section (Figure 1) with cross-sectional area of 2×10 cm for uniform, fully developed, smooth-turbulent flow. The inlet section is followed by a 15-cm-long test section with a 10×15 cm open bottom (the open bottom can accept cores with rectangular cross-section $(10 \times 15$ cm) or circular cross-section (10-cm diameter)). Coring tubes and flume test section, inlet section, and exit sections are constructed of clear polycarbonate materials to permit observation of sediment-water interactions during the course of erosion experiments. The flume includes a port over the test section to provide access to the core surface for physical sampling. The flume accepts sediment cores up to 80-cm in length.

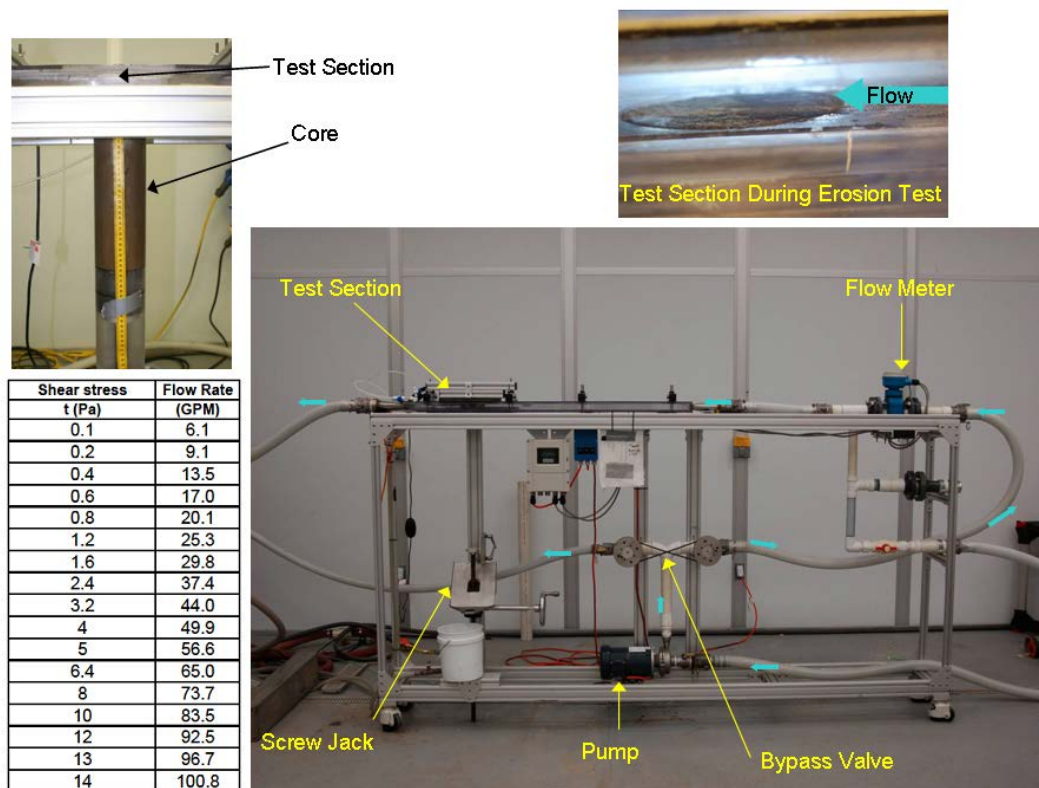| Shear stress t (Pa)	Flow Rate (GPM)
0.1	6.1
0.2	9.1
0.4	13.5
0.6	17.0
0.8	20.1
1.2	25.3
1.6	29.8
2.4	37.4
3.2	44.0
4	49.9
5	56.6
6.4	65.0
8	73.7
10	83.5
12	92.5
13	96.7
14	100.8

Figure 1.   Sedflume erosion flume (lower right). Core inserted into test section (upper left). Core surface flush with bottom of flow channel (upper right). Table of shear stress associated with channel flow rates (lower left).

(3)

Erosion Experiments

Prior to the erosion experiment, descriptions of the core are recorded, including length, condition of the core surface, biological activity, and any visual evidence of layering. Cores are inserted into the testing section of Sedflume and a screw jack is used to advance the plunger such that the core surface becomes flush with the bottom wall of the flume. Flow is directed over the sample by diverting flow from a 5.5-hp trash-pump, through a 5-cm inner diameter hose, into the flume. The flow through the flume produces shear stress on the surface of the core. (Numerical, experimental, and analytical analyses have been performed to relate flowrate to bottom shear stress.) Erosion of the surface sediment is initiated as the shear stress is increased beyond the critical stress for erosion, τ_{cr}. As sediment erodes from the core surface, the operator advances the screw jack to maintain the sediment surface flush with the bottom wall of the erosion flume. Figure 1 includes a photograph of the flume, a close-up photograph of the test section, and a table of flow rate/shear stress relationships.

Erosion rate is determined from the displacement of the core surface over the elapsed time of the experiment. Generally, erosion experiments are performed in repeating sequences of increasing shear stress. Operator experience permits sequencing of erosion tests to allow greater vertical resolution of shear stress/erosion rate data where required. The duration of each erosion experiment at a specified shear stress is dependent on the rate of erosion and generally is between 0.25 and 15 minutes. Shear stresses that induce no measurable erosion are also recorded. The range of shear stress for each cycle is determined by the operator based on the previous erosion sequences and erosion behavior during the ongoing sequence.

Sediment Bulk Properties

Physical samples for bulk sediment property measurements are taken at approximately 3-5 cm intervals during erosion experiments, generally at the end of a shear stress cycle. Physical samples are collected by draining the flume channel, opening the port over the test section, and extracting a sample from the sediment bed. Properties measured include bulk density and grain-size distribution, and separate samples were collected from the core surface for these analyses. These properties strongly influence erosion; therefore, understanding their variation with depth is important in interpreting the erosion data.

Bulk Density Measurements. Bulk sediment density of physical samples is determined by a wet-dry weight analysis. Physical samples are extracted from the saturated core surface and placed in a pre-weighed aluminum tray. Sample weight is recorded immediately after collection and again after a minimum of 12 hours in a 90° C (194° F) drying oven. Wet weight of the sample was calculated by subtracting tare weight from the weight of the sample. The dry weight of the sample was calculated as the tare weight subtracted from the weight after drying. The water content w is then given

$$w = \left(\frac{m_w - m_d}{m_d} \right) \tag{1}$$

where m_w and m_d are the wet and dry weights, respectively. A volume of saturated sediment, V, consists of both solid particles and water and can be written as

$$V = V_s + V_w \tag{2}$$

where V_s is the volume of solid particles and V_w is the volume of water. If the sediment particles

(4)

and water have density ρ_s and ρ_w, respectively, the water content of the sediment can be written as

$$w = \frac{\rho_w V_w}{\rho_s V_s}$$

(3)

A mass balance of the volume of sediment gives

$$\rho V = \rho_s V_s + \rho_w V_w$$

(4)

where ρ is the bulk density of the sediment sample.

Equations (1)-(4) are used to derive an explicit expression for the bulk density of the sediment sample, ρ, as a function of the water content, w, and the densities of the sediment particles and water. This equation is

$$\rho = \rho_s + \frac{w\rho_s(\rho_w - \rho_s)}{\rho_w + w\rho_s}$$

(5)

For the purpose of these calculations, $\rho_s = 2.65$ g·cm^{-3} and ρ_w is calculated for measured pore water at sample temperature.

Particle-Size Distribution. Grain size analysis was performed for each sample collected during erosion experiments at the ERDC Sediment Transport Laboratory. A Malvern Mastersizer 2000 laser diffraction particle-sizer was used to measure the particle-size distributions in sub-samples collected from the cores. The particle sizer measures particle size over the range 0.02 to 2000 μm. Samples were homogenized, sub-sampled (1-2 g), and deflocculated overnight in a solution of sodium metaphosphate (40g/L). Particle size distributions were determined by first removing and sieving (#18 mesh) sediment and shell fragments larger than 1000 μm. The passing portion of the sample was added to the instrument's reservoir and sonicated for 60 seconds prior to analysis. The sample is then pumped and recirculated through the optical module. The optical module includes a spatial filter assembly containing a laser diode and laser beam collimator. The diffraction detector assembly contains a custom photodetector array that is used for the measurement of light scattering by the suspended particles. The distribution of grain sizes and median grain sizes is derived from this light scattering measurement. Organic material was not oxidized before grain size analysis was performed; therefore grain size distributions include organic material less than 1000 μm.

Multivariate Erosion Rate Prediction

The goal of erosion data analysis is to determine appropriate parameterization of erosion processes for numerical modeling studies. For this study, the erosion data are to be described in the SEDZLJ model. SEDZLJ is flexible in the form of the erosion equation, and the effects of bulk density, depth, and applied shear stress may be represented as indicated by the erosion data. Analysis of the erosion data from the Kalamazoo River suggested that the erosion algorithm should be of the following form:

$$\begin{aligned} E &= 0; & (\tau < \tau_c) \\ E &= A\tau^n; & (\tau_c \leq \tau \leq \tau_m) \\ E &= A\tau_m{}^n; & (\tau > \tau_m) \end{aligned}$$

(6)

(5)

where E represents erosion rate (cm·s⁻¹) from the bed, τ is bed shear stress, τ_c is critical stress for erosion, A is an empirical constant, n is an empirical exponent, and τ_m is bed stress at which erosion rate becomes constant. Solution of Equation (6) to data requires solving for three parameters, τ_c, A, and n. Bed stress for the upper limit of erosion rate is determined by examining the data. The best fit of Equation (6) to measured data is accomplished through an iterative, multi-parameter, least-squares method on the linear transform of Equation (6).

Field Experiments

Field experiments were conducted November 6th through 13th, 2013. Field experiments included core collection and cohesive sediment erosion experiments.

Core Collection

On November 06, 2013, nine 10-cm (4-inch) diameter cores were collected from nine locations (Figure 2, Table 1) within the Kalamazoo River for the purpose of erosion experiments. All core collection locations were previously determined and provided to ERDC by the EPA. On November 08, 2013 a core was collected at location SF-4 alt to replace the original SF-4 core. After further review of the core location and visual inspection of the recovered core there was suspicion that the SF-4 core location might have been in a relic channel and EPA requested that a core be collected from the predetermined SF-4 alt location. On November 11, 2013 replacement cores were collected at sites SF-1 and SF-5. While performing a detailed core description back in the mobile laboratory, large vertical fissures were observed in both of the original cores recovered from these locations. These fissures resulted in core failure when trying to introduce the cores to the flume. An additional core was collected from each of the two locations to replace the damaged cores.

A push corer was used to collect all the above mentioned cores. The ERDC push corer is composed of a polycarbonate core barrel, a 4" PVC sleeve, a 2" PVC check valve, and aluminum push poles (Figure 3A). The push corer is lowered by hand to the bottom and vertically driven into the bed by the operator pressing downward on the attached push pole. Care is taken to keep the push pole and core in a vertical orientation during the coring process. The check valve serves to create a seal above the core to prevent the captured sediment core from slipping out of the core tube. Once the core is retrieved to the vessel, a plunger with bentonite paste (for sealing and lubrication) is inserted into the bottom of the core and each end of the core is sealed with end caps (Figures 3B-C). Each core was labeled, logged, and stored submerged in water after collection.
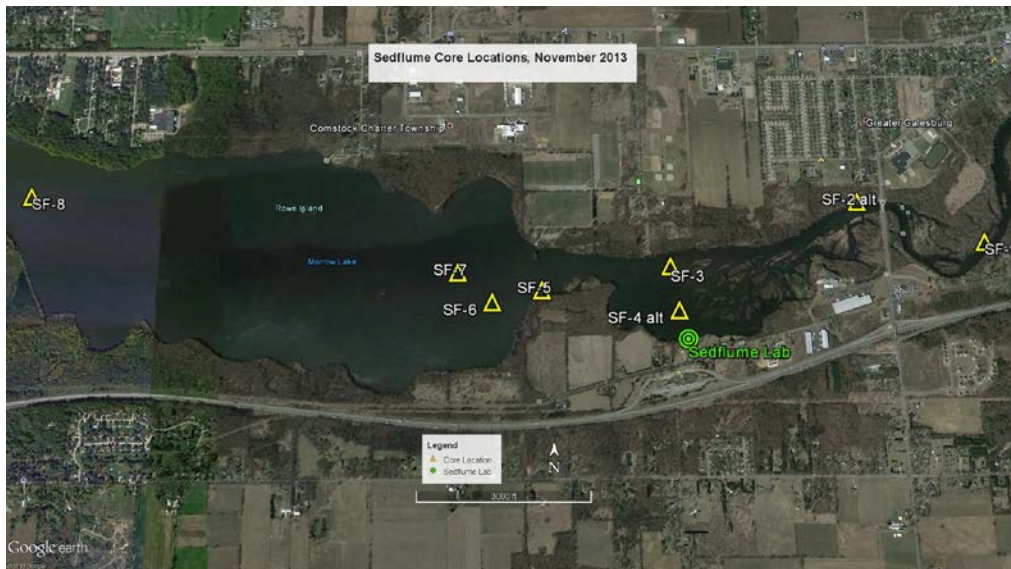
Figure 2 . Sampling locations for Sedflume core collection. Yellow triangles indicate core locations. Green cirlce indicates location of mobile sedflume laboratory. The core location for SF-1 is not indicated on this map. SF-1 was located approximately 20 miles upstream near Battle Creek, MI.

Table 1. Core Summary					
Core ID	Latitude (North)	Longitude (West)	Collection Method	Collection Date	Sample Depth (cm below sediment surface)
SF-1	42.3081	85.1888	Push	11 Nov 2013	31
SF-2alt	42.2803	85.4305	Push	06 Nov 2013	36
SF-3	42.2771	85.4433	Push	06 Nov 2013	26
SF-4alt	42.2746	85.4430	Push	08 Nov 2013	20-21
SF-5	42.2758	85.4519	Push	11 Nov 2013	26-27
SF-6	42.2753	85.4550	Push	06 Nov 2013	24-25
SF-7	42.2769	85.4575	Push	06 Nov 2013	23-24
SF-8	42.2806	85.4864	Push	06 Nov 2013	19-20
SF-9	42.2783	85.4222	Push	06 Nov 2013	30

B) Plungers with Bentonite paste

A) Push Corer

C) Core with plunger inserted.

Figure 3. Sampling devices.

Erosion Experiments

Cores collected were transported by vessel and truck to the ERDC-CHL Field Sediment Laboratory located on the southern shore of the Kalamazoo River in the delta region upstream of Morrow Lake (Figure 2). Erosion experiments were conducted November 7-12, 2013, in the field laboratory following the Sedflume methods presented earlier in this report. During the time of erosion experiments, sediment cores were stored in a shaded barrel, filled with site water.

Results and Discussion

Cohesive sediment transport process data collected during the field study were analyzed to determine SEDZLJ model parameterizations for cohesive sediment erosion. This section presents results of the data analysis, model parameterization, and general observation with discussion. The reader is referred to technical appendices for full presentation of the analyzed dataset.

Cohesive Sediment Erosion

Analysis of cohesive sediment erosion data obtained from undisturbed field cores is inherently complex. Cohesive sediment erosion is sensitive to slight changes in bed density, deposit mineralogy, gas content, organic content, biological activity, debris and a host of other factors. In many cases, these factors change significantly at relatively small vertical scales (such as depositional bed sequences). Consequently, measured cohesive sediment erosion rates from field cores are notoriously variable. To counter the large variance in measured erosion rates, field erosion experiments are conducted in a manner to produce a large sample from which to derive statistically representative relationships for various numerical erosion algorithms. To ensure high quality in the data analysis, data and associated experimental notes are evaluated to identify outliers in the dataset. Outliers are rejected based on comparisons between adjacent data points and experimental log notes.

During sediment erosion tests, cores SF-6 and SF-9 developed fissures that resulted in rapid erosion and core failure. Usable data were collected down to a depth of approximately 10 cm prior to fissure development. However, due to the loss of the core integrity after fissure development no usable erosion data could be collected below 10 cm.

Erosion testing revealed all cores to be notably layered. Consequently, erosion datasets from the core stations were segmented by bed layers as seen in Figure 4. Layer segmentation during analysis was based on visual core descriptions logged in the field, physical sampling, erosion experiment notes, and erosion rate data. Core descriptions including photographs, visual descriptions, and results of physical sample analysis are provided in Appendix A. Figures that identify bed layers for cores are provided in Appendix B.
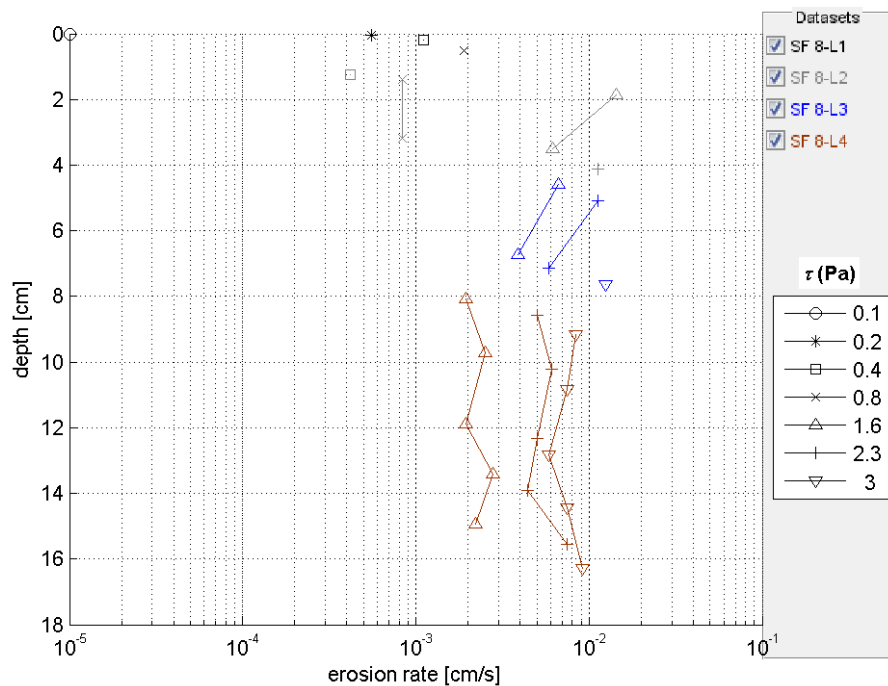

Figure 4. Plot depicting the change in erosion rate with depth for core SF-8. Colors indicate bed layers, symbols indicate applied shear stress.

(9)

Erosion Parameterization

Erosion rate data were evaluated for relationships between erosion rate and applied shear stress. As mentioned previously, each of the analyzed cores indicated bed layering. In some instances, boundaries between layers were very distinct; in other cases transitions between bed layers were more gradual. Each of the identified sediment layers within a core were first analyzed separately. When appropriate, bed layers were combined with adjacent layers to form groupings that contain a larger number of erosion data points.

In general, it was observed that erosion rates decreased with depth down core. Erosion data from core SF-8 will be presented to illustrate this pattern. Erosion data from all cores collected can be found in Appendix B. As seen in Figure 4, erosion rates at individual applied shear stresses tend to decrease with depth. This is best seen at a shear stress of 1.6 Pa, which starts with an erosion rate of 0.015 cm/s at a depth of 2 cm, but decreases by nearly an order of magnitude to .002 cm/s at a depth of 15cm. While the magnitude of change was found to be smaller for other shear stresses tested in SF-8, the trend of decreasing erosion rates with depth was observed.

Multivariate least square fit of erosion rate to shear stress for SF-8 is presented in Figures 5-7. Each figure depicts the best fit to Equation 6 for a discrete region of the core. The core was divided into three distinct regions for erosion parameterization; top, middle, and bottom. Bed layers 1 and 4 both displayed distinct boundaries from adjacent bed layers and were therefore identified as the top and bottom of the core, respectively. In contrast layers 2 and 3 had gradual boundaries between them. Layers 2 and 3were combined and the best fit line for Equation 6 matched the data points reasonably well (Figure 6). For that reason these two layers were identified as the middle section of the core. Table 2 shows the grouping of layers for each core and the resulting erosion parameters for each group.
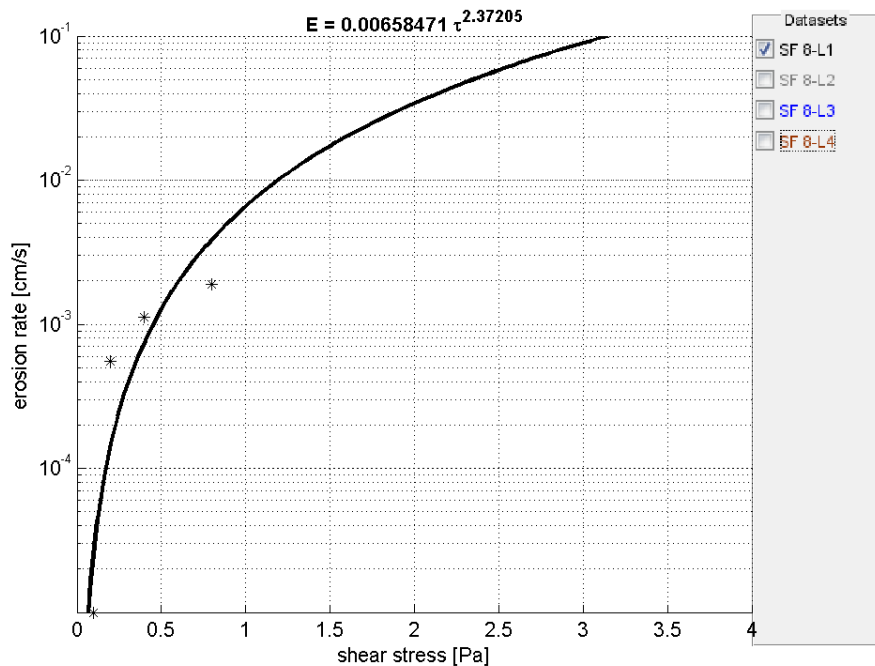

$$E = 0.00658471\,\tau^{2.37205}$$

Figure 5. Erosion rate data and best fit line to Equation 6 for the top of core SF-8. Datasets included in the analysis are indicated on the right (with check mark), and symbol color corresponds to text color of the dataset.
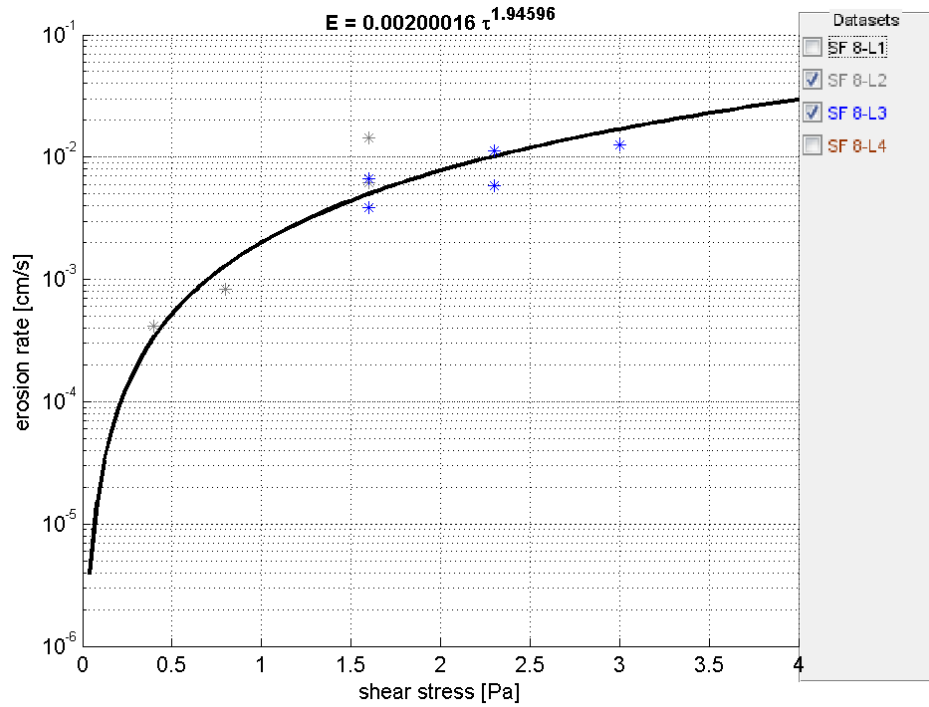
(10)

$$E = 0.00200016\,\tau^{1.94596}$$

Figure 6. Erosion rate data and best fit line to Equation 6 for the middle of core SF-8. Datasets included in the analysis are indicated on the right (with check mark), and symbol color corresponds to text color of the dataset.
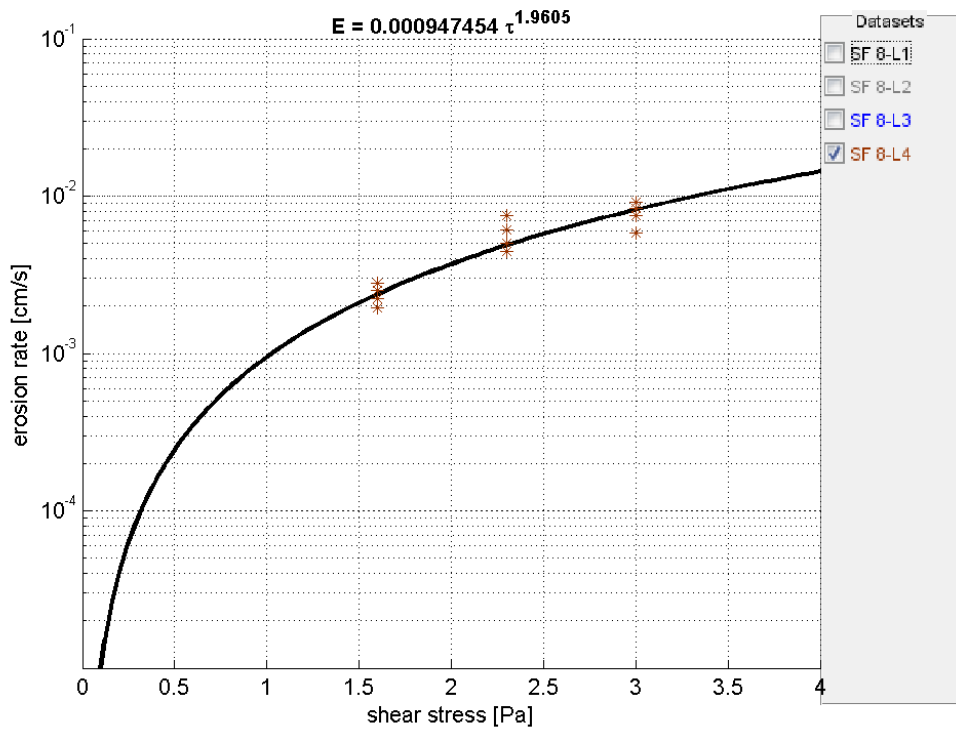

$$E = 0.000947454\,\tau^{1.9605}$$

Figure 7. Erosion rate data and best fit line to Equation 6 for the bottom of core SF-8. Datasets included in the analysis are indicated on the right (with check mark), and symbol color corresponds to text color of the dataset.

(11)

Table 2. Cohesive Erosion Parameterization for SEDZLJ					
Core	Depth	τ_c	τ_m	A	n
	(cm)	(Pa)	(Pa)		
SF1-Top (L1,L2)	<5	0.1	1.6	1.24E-02	2.74
SF1-Middle (L3)	5-13	0.4	1.5	7.07E-03	2.66
SF1-Middle (L4)	13-21	0.8	2.5	1.99E-03	2.49
SF1-Bottom (L5)	>21	1.0	3.5	4.84E-04	2.98
SF2-Top (L1,L2)	<6	0.1	0.9	2.79E-02	2.81
SF2-Middle (L3,L4)	7-17	0.2	1.6	6.85E-03	2.06
SF2-Bottom (L5)	>20	Noncohesive Sand Layer			
SF3 (L1,L2,L3,L4,L5)	0-21	0.2	1.3	8.62E-03	3.16
SF4-Top (L1)	<1	0.1	0.8	3.60E-02	3.15
SF4-Middle (L2)	2-4	0.2	2	4.44E-03	2.08
SF4-Bottom (L3)	>4	Noncohesive Sand and Wood Layer			
SF5-Top (L1,L2)	<5.5	0.1	1.0	1.96E-02	2.82
SF5-Middle (L3,L4)	5.5-14.5	0.4	3	5.17E-03	1.15
SF5-Bottom (L5)	>14.5	0.8	3	1.05E-03	2.62
SF6-Top (L1)	<2	0.2	0.6	3.92E-02	2.77
SF6-Bottom (L2,L3)	2-10.5	0.2	1.5	6.54E-03	2.77
SF7-Top (L1)	<1	0.1	2.25	8.51E-03	1.08
SF7-Middle (L2)	1-3.5	0.4	2.0	2.14E-03	3.18
SF7-Bottom (L3,L4)	>3.5	0.8	3.2	1.42E-03	2.28
SF8-Top (L1)	<1	0.1	1.6	6.58E-03	2.37
SF8-Middle (L2,L3)	1-8	0.2	3.2	2.00E-03	1.94
SF8-Bottom (L4)	>8	1.2	4	9.47E-04	1.96
SF9-Top (L1)	<1	0.1	1	1.82E-02	1.90
SF9-Middle (L2)	1-8.5	0.4	2.25	5.03E-03	1.68
SF9-Bottom (L3)	>8.5	0.8	2.5	1.47E-03	2.91

After grouping layers and performing the least squares fit to Equation 6, uncertainty confidence intervals were determined. The 90% confidence intervals on the data and of the A and n components of the fit parameter Equation 6 were determined. Additionaly, the standard error of the mean (SEM) at 90% confidence was also calculated. Figure 8 shows these uncertainties plotted for the middle section of core SF-8. The confidence interval of the data ("ci data") demonstrates the interval within which additional data points would fall with 90% confidence. The confidence interval of the parameters ("ci fit param") describes the variation in a parameter that corresponds to the confidence limits of the data. The SEM describes the confidence limits of the best fit line. That is to say that if additional data points were placed in the set, the fit line would be expected to fall within this range at 90% confidence.

(12)

The number of data points in each grouping (N), the coefficient of determination (r^2) and p-value (p) are shown at the top of Figure 8. The r^2 value is used to determine how close the data points fit the regression. In this case 86% of the data points can be explained by the regression. The p-value indicates the probability of obtaining the r^2 value by pure chance. In this case, the p-value of 3.75e-05 indicates that there is very little chance that the r^2 value of 0.86 is due to chance. Typically when p<0.05 the test statistic is considered significant. This is the case for the middle section of core SF-8. The regression indicates that 86% of the data points are explained by the resulting fit and the p-value indicates that there is a very low probability that this result is due to chance. The range of the *A* parameters for both the SEM and fit parameter confidence interval, along with then N for all the groupings in each core are listed in Table 3. Due to small degrees of freedom, no values were reported for groupings that had N values ≤4.
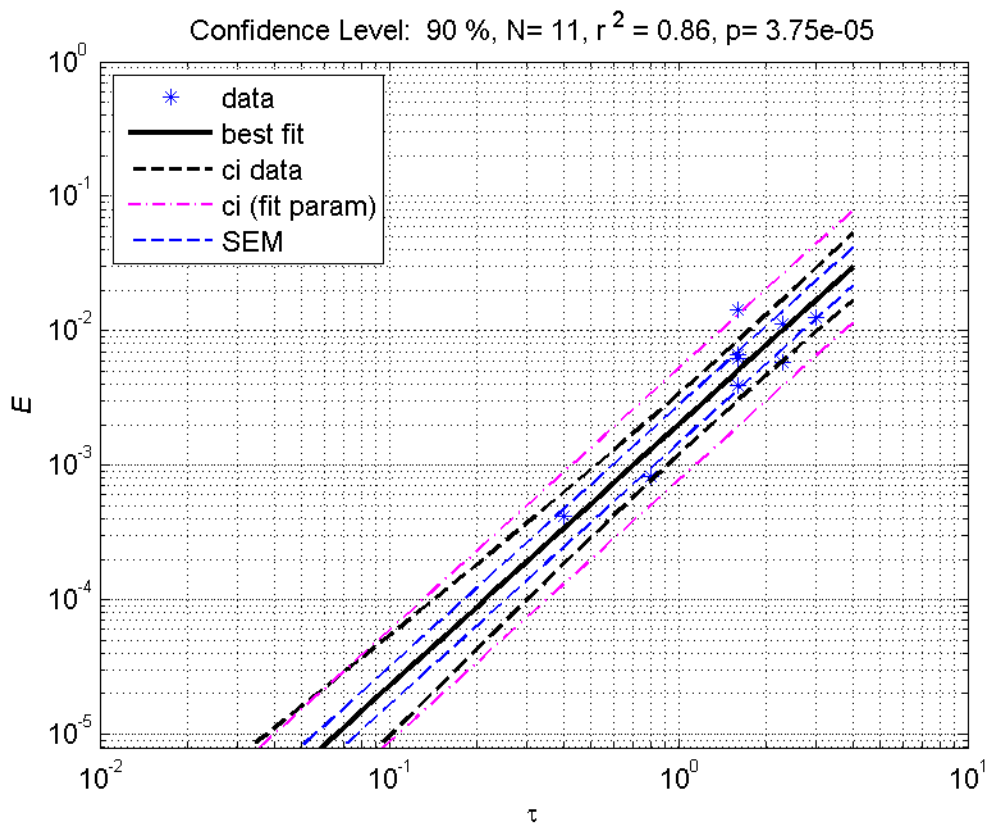

Figure 8. Erosion parameterization uncertainties for the middle section of core SF-8 (L2 & L3). Shear stress (τ) in Pa and erosion rate (E) in cm/s are plotted on the x and y axis, respectively. The best fit to Equation 6, 90% confidence intervals on the data ("ci data"), 90% confidence intervals on the fit parameters ("ci (fit param)"), and standard error of the mean at 90% ("SEM") are provided. The sample size (N), r^2, and p-value are displayed at the top of the figure.

Table 3. Cohesive Erosion Parameterization Uncertanties						
Core	Depth	N	A (SE 90%)		A (CI Param 90%)	
	(cm)		low	high	low	high
SF1-Top (L1,L2)	<5	12	7.02E-03	2.20E-02	2.84E-03	5.43E-02
SF1-Middle (L3)	5-13	13	5.41E-03	9.22E-03	2.87E-03	1.74E-02
SF1-Middle (L4)	13-21	13	1.53E-03	2.59E-03	1.19E-03	3.32E-03
SF1-Bottom (L5)	>21	12	2.83E-04	8.26E-04	1.86E-04	3.32E-03
SF2-Top (L1,L2)	<6	13	1.38E-02	5.62E-02	5.36E-03	1.45E-01
SF2-Middle (L3,L4)	7-17	18	6.08E-03	7.73E-03	4.06E-03	1.16E-02
SF2-Bottom (L5)	>20	N/A	Noncohesive Sand Layer			
SF3 (L1,L2,L3,L4,L5)	0-21	33	6.65E-03	1.12E-02	2.33E-03	3.19E-02
SF4-Top (L1)	<1	4	-	-	-	-
SF4-Middle (L2)	2-4	5	1.57E-03	1.26E-02	4.32E-04	4.56E-02
SF4-Bottom (L3)	>4	N/A	Noncohesive Sand Layer			
SF5-Top (L1,L2)	<5.5	11	1.10E-02	3.48E-02	4.80E-03	8.01E-02
SF5-Middle (L3,L4)	5.5-14.5	15	4.10E-03	6.51E-03	2.05E-03	1.30E-02
SF5-Bottom (L5)	>14.5	11	7.06E-04	1.55E-03	5.19E-04	2.12E-03
SF6-Top (L1)	<2	3	-	-	-	-
SF6-Bottom (L2,L3)	2-10.5	14	5.08E-03	8.46E-03	2.53E-03	1.69E-02
SF7-Top (L1)	<1	3	-	-	-	-
SF7-Middle (L2)	1-3.5	5	1.56E-03	2.92E-03	1.05E-03	4.36E-03
SF7-Bottom (L3,L4)	>3.5	29	1.29E-03	1.56E-03	1.09E-03	1.84E-03
SF8-Top (L1)	<1	4	-	-	-	-
SF8-Middle (L2,L3)	1-8	11	1.44E-03	2.77E-03	7.68E-04	5.21E-03
SF8-Bottom (L4)	>8	15	7.05E-04	1.27E-03	6.00E-04	1.50E-03
SF9-Top (L1)	<1	4	-	-	-	-
SF9-Middle (L2)	1-8.5	12	4.53E-03	5.58E-03	3.59E-03	7.05E-03
SF9-Bottom (L3)	>8.5	3	-	-	-	-

Cores SF-2 and SF-4 were the only cores to have bed layers with higher erosion rates at the core bottom. In both instances this was associated with non-cohesive sand at the bottom (Appendix A and Table 2). It should be noted that SF-6 did show a layer of sandy material and

(14)

high erosion rates at a depth of approximately 10 cm, however, unlike cores SF-2 and SF-4 this sandy layer was not located at the bottom of the core. As stated previously, Core SF-6 failed due to fissure development and prevented further erosion and grain size analysis of the remainder of the core. Therefore, it is unknown whether the sandy material seen at approximately 10-12 cm depth persisted throughout the remainder of the core, or if it was a sandy layer within an otherwise more cohesive core. While all the above cores did have elevated erosion rates associated with non-cohesive layers, it was observed that erosion rates generally decreased with depth.

Critical shear stress increased with depth below the sediment water interface for each core with the exception of SF-6 (Table 2). Core SF-6 only had erosion data down to approximately 10 cm and critical shear stress was found to be constant over that depth. Critical shear stress may have been greater for sediments buried deeper than 10 cm. This trend along with the decrease in erosion rate with depth is expected for cohesive sediments. Cohesive sediments typically have a trend of increasing density with depth due to self-weight consolidation. Consolidation produces stronger, more frequent bonds between particles. It should be noted that density does not increase consistently with depth due to natural variation in multiple other sediment properties. However, the general trend for the Kalamazoo River cores does indicate increasing density with depth. Density profiles for individual cores are presented in Appendix A.

Summary and Conclusions

The EPA commissioned the ERDC to conduct cohesive sediment erosion testing services for the purpose of defining erosion rates of oil contaminated sediments in the Kalamazoo River near Marshall, MI. ERDC-CHL conducted the erosion testing in November 2013.

Nine, 4-inch (10-cm) diameter sediment cores were collected in a reach of the Kalamazoo River (in the vicinity of Marshall, MI). The cores were eroded in the Field Sediment Transport Laboratory that was operated on the southern shore of the Kalamazoo River in the delta region upstream of Morrow Lake. During erosion experiments, the cores were visually described, eroded, and subsampled for physical properties. No sheen or other visible sign of oil contamination was observed on the sediments or in the overlying water during core collection or erosion testing. Observations during the erosion experiments indicated that all cores were notably layered. No clear trends were seen between cores based on geographical location, however, all cores were found to have decreasing erosion rates and increasing critical shear stress with depth. Erosion data were analyzed by core and depth groups and empirical coefficients were determined for modeling the system with SEDZLJ. Uncertainties of these parameters were also calculated and provided. It is suggested that the SEM 90% be the primary source of uncertainty utilized for modeling, as it reflects the range the best fit line would fall in if data points were added to the set. It is our recommendation that the 90% confidence interval of the fit parameters should be utilized only as a secondary level of uncertainty.

Acknowledgements

References

McNeil, J., Taylor, C., and Lick, W. 1996. 'Measurements of erosion of undisturbed bottom
   sediments with depth', *Journal of Hydraulic Engineering*, 122(6), 316-324.